Current Advancements in Material Research and Techniques Focusing on Lead-free Perovskite Solar Cells

CL-170345 Received: April 9, 2017 | Accepted: May 2, 2017 | Web Released: May 12, 2017

Highlight Review

Current Advancements in Material Research and Techniques Focusing on Lead-free Perovskite Solar Cells

Chu Zhang,[2] Liguo Gao,*[1] Shuzi Hayase,[2] and Tingli Ma*[2]

[1]School of Petroleum and Chemical Engineering, Dalian University of Technology, Panjin Campus, Panjin 124221, P. R. China

[2]Graduate School of Life Science and Systems Engineering, Kyushu Institute of Technology, Kitakyushu, Fukuoka 808-0196

(E-mail: liguo.gao@dlut.edu.cn)

Dr. Liguo Gao graduated from Jilin University. Now he is working at Dalian University of Technology. His interests include researching on integrating silicon solar cell with perovskite solar cell, developing novel architecture for perovskite solar cells, and photoelectrochemical systems such as fabricating photoanodes by nanoepitaxy TiO_2 on Si substrate for solar water splitting.

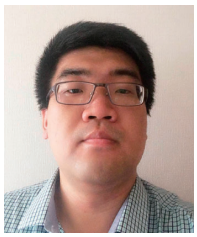

Chu Zhang is a Ph.D. candidate of Tingli Ma's Lab, Kyushu Institute of Technology. He received bachelor's degree from Sun Yat-Sen University in 2010, and master's degree from Oregon State University in 2014. His current research field is focused on Pb-free perovskite material and the perovskite solar cell devices.

Dr. Tingli Ma received her Ph.D. degree in 1999 from Department of Chemistry, Faculty of Science of Kyushu University, Japan. She then joined the National Institute of Advanced Industrial Science and Technology (AIST) as a Special Postdoctoral Researcher from 1999 to 2004. She moved to the Dalian University of Technology, China in 2007. She is working at the Graduate School of Life Science and Systems Engineering Kyushu Institute of Technology, Japan since 2014. She leads research teams studying on inorganic and organic solar cell, such as dye-sensitized solar cells and perovskite solar cell, and other related projects including development of catalysts, hydrogen production, functional dyes and nano semiconductor materials. Dr. Ma has published more than 100 papers in peer-reviewed journals.

Shuzi Hayase graduated from Osaka University in 1978 and received Ph.D. from Osaka University in 1983. He joined R&D Center in Toshiba from 1978 to 2000, during which the author was engaged in development of ULSI lithography, solar cells, direct methanol fuel cells, and polysilanes. He joined polysilane research in Robert West group of Wisconsin University (US) from 1988 to 1990. He is a professor of Kyushu Institute of Technology (National Institute) since 2001. From 2009 to 2017, he was a Supervisor of PRESTO project (Japan Science and Technology Agency (JST), "Photoenergy conversion systems and materials for the next generation solar cells" project). From 2012 to 2016, he was Dean of graduate school of life science and systems engineering, Kyushu Institute of Technology. Since 2016 he is Executive Director, vice-President of Kyushu Institute of Technology. His research interest is printable solar cells.

Abstract

Organic–inorganic lead halide perovskite solar cells (PSCs) recently achieved a photo-to-electricity conversion efficiency (PCE) of 22.1%. They drew much attention as promising photovoltaic devices. However, the Pb-based PSCs face great challenges for commercial and industrial applications due to the instability and the toxicity of perovskite materials. Herein, we summarize the current development of various types of Pb-free perovskites, such as the Sn-, Bi-, Ge-, Sr-, and Cu-based perovskites and their devices. In addition, we will address some remaining issues and prospects of the Pb-free PSCs.

Keywords: Perovskite solar cell | Pb free | Organic–inorganic hybrid material

1. Introduction

The organic–inorganic lead halide perovskite solar cell (PSC) has drawn much attention due to its unique advantages and rapid progress.[1–5] Researches have demonstrated that the Pb-based perovskite materials exhibit the characteristic strong absorption across a wide spectrum range,[6] as well as a long carrier diffusion length for both the electrons and holes.[7] Another advantage is that the PSC device does not require relatively extreme conditions such as a high temperature and high pressure, which are normally required during silicon-based solar cell fabrication. Such advantages would result in low manufacturing costs and easily satisfied industrial operating requirements. In addition, the raw materials, such as PbI_2 and methylammonium iodide (MAI), also have cost advantages compared to silicon-based solar cells.

Despite the exciting advantages mentioned above, the Pb-based PSCs still have several serious issues. One main issue is its toxicity. A study showed that Pb affects the human nervous system as well as the reproductive system.[8] Due to the easy decomposition of the perovskite materials in a humid environment or under strong UV radiation, the processor would produce Pb^{2+} cations. In addition, the decomposition procedure of the perovskite is irreversible. Another issue is an efficiency drop or device failure, which causes defects on the TiO_2 surface.[9,10] When under an oxygen-rich environment, UV light can significantly promote the inducement of oxygen molecule diffusion into the perovskite layer and form peroxide or superoxide compounds, which produce some defects on the TiO_2 surface. It has also been shown that UV illumination alone can encourage carrier recombination at the local trapping sites, as well as promoting halogen radicals, thus causing degradation.[11] Moisture and high temperature are the most hazardous factors to the PSCs, because Pb-based perovskite materials would exhibit degradation under the conditions of both moisture and high temperature over 140 °C.

In order to solve these key issues mentioned above, many groups carried out studies, including the development of Pb-free materials for PSCs. In this review, we will introduce the very recent progress in the development of Pb-free materials and applications for PSCs. We will also state the remaining issues and prospects of Pb-free perovskite materials.

2. Sn-based Perovskite

When considering the reduction or replacement of Pb, Sn turned out to be the primary choice. Being in the same group as Pb, the Sn perovskite is predicted to be able to maintain most of the optoelectronic properties of the Pb perovskite due to similar band structures,[12] and to avoid the toxicity and pollution issue of lead.

In order to utilize Sn for the light absorber, attempts of partial and full replacement of Pb by Sn were both carried out.[13] In 2014, our group reported a series of Pb/Sn hybrid PSCs, which achieved promising power conversion efficiencies (PCEs) over 4%.[14] We also found that the absorption edge of the mixed perovskite was especially pushed up to the NIR range of 1060 nm, much longer than that of Pb perovskite (below 800 nm). It was also shown that when the ratio of Pb/Sn reached 1:1 ($MAPb_{0.5}Sn_{0.5}I_3$), the highest PCE of 4.18% was achieved with the open circuit voltage (V_{oc}) = 0.32 V, short-circuit current density (J_{sc}) = 19.88 mA cm^{-2}, and fill factor (FF) = 0.37.

Figure 1 showed the band structure and absorption spectra of these Pb/Sn mixed perovskites showing different band structures under the various Sn/Pb ratios. In 2016, Lin et al. also reported the especially wide absorption range of $MASn_{0.5}Pb_{0.5}I_3$. By introducing fullerene as the electron-transfer material, they achieved a higher V_{oc} of 0.69 V, thus pushing the PCE up to 10%.[15]

Other groups have also studied the hybrid Pb/Sn-based PSCs. Hao et al. reported a mixed $CH_3NH_3Sn_{0.25}Pb_{0.75}I_3$ perovskite with the PCE of 7.37%,[16] and the J_{sc} is higher than that of $MAPbI_3$. Zuo et al. also found that adding Sn to the Pb-based perovskite could enlarge the perovskite crystal grain, improve the surface coverage, and reduce the local traps. They achieved a PCE of 10.1% for the Pb/Sn mixed perovskite.[17]

Normally, we would consider that with a higher lead ratio comes better PCE, but Jen and co-workers showed that other cations/anions also play important roles. They achieved 9.77% with a $MASn_{0.15}Pb_{0.85}I_{3-y}Cl_y$ (band gap of 1.38 eV) device, and 14.35% with a devise with a lower lead ratio, i.e., $MA_{0.5}FA_{0.5}Pb_{0.75}Sn_{0.25}I_3$ (band gap of 1.33 eV).[17,18]

It also appeared that the inverted structure would result in better performance with Sn/Pb mixed materials. For example, in 2016, Li et al. fabricated an inverted structured device with $MAPb_{0.5}Sn_{0.5}I_3$, achieved a PCE of 13.6%.[19] Liao et al.

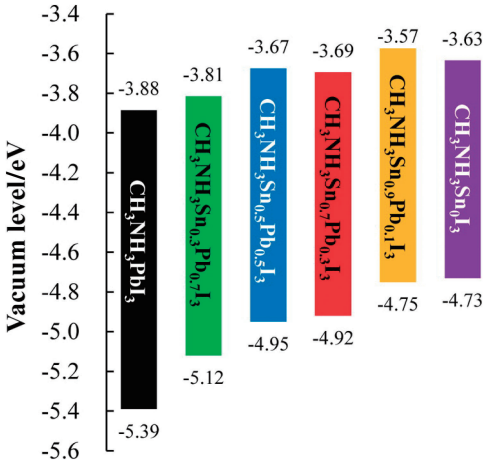

Figure 1. Band structure and absorptions of Sn/Pb mixed perovskite.[14]

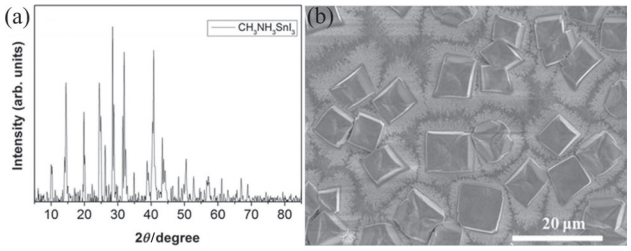

Figure 2. XRD (a) and SEM (b) images of $MASnI_3$ perovskite.[21]

employed $(MAPbI_3)_{0.4}(FASnI_3)_{0.6}$ in inverted device and achieved a PCE of 15.08%.[20]

In 2014, Noel et al. reported fully substituted Sn perovskite $MASnI_3$, revealing that the Sn perovskite needed no further annealing to achieve a crystalline structure.[21] However, their study also revealed that the Sn perovskites have a relatively short carrier lifetime and a much shorter carrier diffusion length than the Pb-based perovskites. This suggested that stronger electron and hole extracting materials would be necessary. The band gap of this perovskite was estimated to be 1.23 eV, the device V_{oc} was 0.88 V, and the PCE was 6.5%. Figure 2 showed the XRD pattern and the SEM image of this Sn perovskite. Other studies of fully substitute Sn perovskites were also reported. For example, Liao et al. reported a $FASnI_3$ device with the best PCE of 6.22%.[22]

It should be pointed out that the Sn-based perovskite still had the instability issue. When the Sn-based perovskite was exposed to a humid environment or a high temperature (over 50 °C), the Sn^{2+} cations could be oxidized into Sn^{4+} cations relatively fast, resulting in a sharp decrease in the PCE. It has been shown that the stability of the Sn perovskites was lower than that of the Pb perovskite.[14]

In order to improve the stability of the Sn perovskite, many studies were carried out to modify the fabricating techniques. One way to improve its stability is to introduce certain oxidation suppressors to reduce tin vacancies and Sn^{4+} formation, and mostly, such materials are tin halides. Lee et al. reported that a combining treatment of SnF_2 and pyrazine can result in a compact and smooth $FASnI_3$ film surface, improving the PCE from 2.8% to 4.0%.[23] Song et al. introduced SnI_2 to treat $ASnI_3$ (A = Cs, MA, FA) to suppress Sn^{2+} vacancies, achieve a PCE of 4.81%.[24] Yokoyama et al. proposed that the tin halide additives could supply SnO_2 or SnOH to promote the hole carrier density and suppress the oxidation of the perovskite materials.[25]

Many other methods were introduced to enhance the stability of tin-based perovskite device. Jung et al. carried out consequential vapor deposition under a high vacuum (1.5×10^{-6} Torr) condition to synthesize $MASnBr_3$, obtaining a well-uniformed perovskite film of 400 nm thickness and achieving a PCE of 1.12%.[26] Yokoyama et al. introduced low-temperature vapor deposition (LTVD) technique in combination with low-temperature annealing to fabricate a dense $MASnI_3$ film, achieving a PCE of 1.86%.[27] Fujihara et al. employed an anti-solvent method to fabricate $MASnI_3$ devices, achieving an improved coverage, with an average PCE of 2.14%.[28]

The Sn-based perovskite has become a promising alternative material for replacing the Pb-based perovskite. However, instability and low PCE issues of the materials and devices still remain. In addition, Sn-based perovskite also has a certain degree of toxicity. Recently, Babayigit et al. systematically studied the environmental impact of the Pb- and Sn-based perovskites by using the zebrafish (*Danio Rerio*) as the model organism. By comparing the damage done to living organic samples, they showed that the Sn-based perovskite also possesses a significant degree of toxicity.[29] Such problems prompt more research to find other alternative materials, which can be more stable with less or no toxicity.

3. Bi-based Perovskites

The Bi cation is non-toxic with a stable 6p-block structure and a high dielectric constant. Bi halides are also predicted to have an octahedral-coordinated structure as one class of defect-tolerant materials, suggesting that the Bi-based perovskite can exhibit a longer charge carrier lifetime by having lower intrinsic trap densities and defect states.[30] Therefore, Bi-based perovskites have been paid much attention as a promising candidate Pb-free perovskite.

Bi-based perovskites entered the scene in 2015, when Park et al. synthesized the Bi-based perovskite $A_3Bi_2I_9$ (A to be Cs and MA) as a photovoltaic absorber.[31] Their XRD results for the Bi-based perovskites with different halogen anions showed that these Bi perovskites had similar hexagonal crystalline phase structures. They estimated the band gap of $A_3Bi_2I_9$ to be ca. 2.1 eV for MA and 2.2 eV for Cs, and the exciton binding energy was calculated to be 70 meV (while Pb perovskite is at 25–50 meV). They obtained a low PCE of 1.09% for $CS_3Bi_2I_9$ (FF = 0.6, $V_{oc} = 0.85$ V, and $J_{sc} = 2.15$ mA cm^{-2}), 0.12% for $MA_3Bi_2I_9$ (FF = 0.33, $V_{oc} = 0.68$ V, and $J_{sc} = 0.52$ mA cm^{-2}). The low efficiency could be due to several reasons, such as extra band-gap states, poor morphology, excess reactant residue, and interface contact. They also tested the stability of $MA_3Bi_2I_9$. While stored under dry and dark conditions, the Bi perovskites showed no significant change in their optoelectronic properties for one month. These results suggested that the Bi perovskite has the potential of good stability.

Later in 2015, Hoye et al. synthesized the pure-phase Bi halide perovskite $MA_3Bi_2I_9$ (MBI) using both solution processing and vapor-assisted techniques.[32] Such methods produced a Bi perovskite with the band gap of 2.0 eV. The optical absorption coefficient was estimated to be ca. 10^5 cm^{-1}. They also studied the carrier lifetime of the Bi perovskites using photoluminescence (PL) decay under the ambient room temperature. By using a two-step spin-coating method and employing MAI in the vapor phase rather than in the liquid phase, the surface morphology of the MBI was improved, producing a smoother film, pure phase, and dramatically increasing the PL decay time from 0.12 to 0.76 ns. They also found that the vapor processing rather than the solution processing was the method that achieved longer PL decay times. They obtained the PL decay times of at least 760 ps with the bulk lifetime closer to 5.6 ns. They also demonstrated that $MA_3Bi_2I_9$ did not decompose into BiI_3; instead, it formed an oxidation layer in a humid environment. Under the condition of ca. 61% relative humidity and ca. 22 °C, the XRD showed that the Bi perovskite lasted 25 days with a minimal structural change, while the Pb-based perovskite readily decomposed after only 5 days. Their results showed that the Bi perovskite is a promising material for solar absorbers.

In order to obtain an in-depth understanding of the crystal structure of the Bi-based perovskite, Eckhardt et al. recently performed a crystallographic study to gain insight into the Bi perovskite.[33] They synthesized the $MA_3Bi_2I_9$ single crystal via the solution process and found that the anion group $(Bi_2I_9)^{3-}$ in $MA_3Bi_2I_9$ forms face-sharing octahedron pairs separated by MA^+ ions in contrast to the corner-sharing structure of $MAPbI_3$. The octahedron structure formed by the Bi–I bonds also showed a minor distortion, which was suggested to be caused by an inner repulsion between the two Bi^{3+} ions. This suggests that the structure is a 2D hexagonal shape. The 2D layered crystal structure can explain the reason that the Bi perovskite is more stable than the Sn and Pb perovskites.

Studies were also done with Bi perovskites to obtain an improvement by switching MA with inorganic cations and by partially replacing halogen with other chalcogenide elements. A series of ambient stable $MABiXY_2$ types of Bi perovskite structures were predicted by Sun et al.,[34] using the split-anion method with the density functional theory (DFT) and spin–orbit coupling (SOC) calculations, where X = chalcogenides (S, Se, Te) and Y = halogens (I, Br, Cl). They estimated that the lowest band gap was 1.24 eV ($MABiTeI_2$), and the highest one was 2.00 eV ($MABiSCl_2$), compared to that of $MAPbI_3$ (1.55 eV) in previous calculations and experiments.[35] Figure 3 showed the calculated band gaps of these mixed-anion Bi perovskites. They also suggested that $MABiSI_2$ (band gap = 1.38 eV) had a better absorption below 3 eV, which consisted of about 94% radiation under the AM 1.5 condition. Though the PCE was not emphasized here, the good optoelectronic properties of $MABiSI_2$ still proposed a rather strong photovoltaic potential. In addition, they also indicated that the split-anion method could be used to find a possible solution to the degradation issue of the Sn perovskite.

However, such a theoretical prediction should be considered with careful practical validation. A recent report demonstrated that the Bi perovskites with a chalcogenide/halogen anion mixture exhibited a certain level of thermodynamic instability, which may result in decomposition and losing the perovskite structure, or prevent the formation of the 3D perovskite lattice.[36] In this attempt, although the tolerance factor (t) was in good agreement with that of the theoretically stable perovskite material, the difference in the ion radii and electronegativity still caused a significant phase segregation, and none of the several trials with different compositions succeeded in forming the target perovskites. Research concerning such topics is very limited, and further in-depth investigations are still necessary. If there is indeed a way to fabricate a chalcogenide-doped Bi perovskite, which is thermodynamically stable, it could well be one of the most promising substitutes for the Pb perovskite.

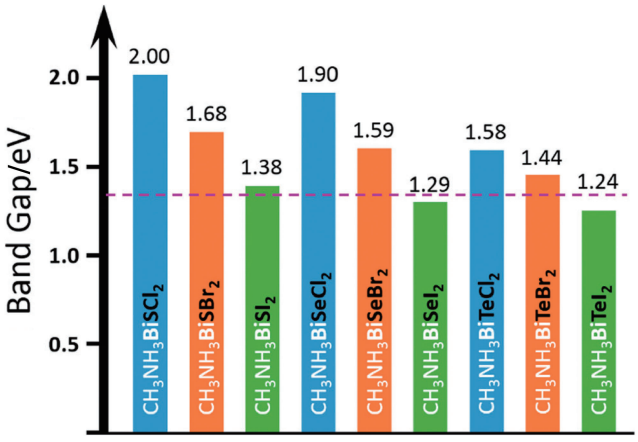

Figure 3. Theoretical estimated band gaps of mixed anion Bi-based perovskite.[34]

Some post-treatment methods were also introduced to try to refine the morphology of the bismuth-based perovskite film. Kulkarni et al. tried to treat the film with NMP to get better surface coverage, improving PCE from 0.19% to 0.31%.[37] Okano et al. fabricated the MBI perovskite device with N_2 gas blowing to the film during spin coating. This method greatly improved the coverage of the MBI film, enhancing the PCE from 0.07% to 0.08%.[38] Ran et al. employed a thermal evaporation-assisted deposition technique to fabricate the MBI film, achieving a PCE of 0.39% with an exceptional high V_{oc} of 0.8 V on an inverted device.[39]

Another idea of Bi substitution is to form a double perovskite with Bi and another cation. Xiao et al. carried out a comprehensive theoretical study focusing on this type of materials.[40] The study showed that the bismuth-based double perovskite $AMBiX_6$, also known as the "elpasolite" material, is predicted to have a good stability against both head and moisture, with a long carrier recombination lifetime and a low carrier effective mass. The issue is, although many elements can fit in the formula as the candidates for A and M sites, very few of them are predicted to be able to sustain the double perovskite structure under room temperature. Most of the combinations would be either hard to synthesize or existed only at a higher temperature as a meta-stable form.

Two attempts recently reported by Volonakis et al.[41] and Slavney et al.[42] suggested that silver might be a superior choice on the M site. In these reports, the cations of the noble metals Cu, Ag, and Au were theoretically considered. They synthesized double perovskites $Cs_2BiAgCl_6$ and $Cs_2BiAgBr_6$. The indirect band gaps of the obtained $Cs_2BiAgCl_6$ and $Cs_2BiAgBr_6$ perovskites were determined to be 2.3–2.5 and 1.95 eV, respectively. Especially, Slavney et al. pointed out that their $Cs_2BiAgBr_2$ perovskite has a uniquely long PL decay time of over 600 ns, and their results suggested that the Bi-based double perovskites could generally have a longer carrier lifetime. Filip et al. carried out a theoretical study to confirmed the band gap of Cs_2AgBiX_6 (X = Cl, Br) to be near 2 eV. The study also suggested that Cs_2AgBiI_6 can hardly constrain its double perovskite structure under room temperature and thus will be hard to synthesize.[43] Wei et al. introduced an organic cation to synthesize the double perovskite material MA_2KBiCl_6[44] and $MA_2AgBiBr_6$,[45] showing that the hybrid double perovskite is also viable. However, tests showed that the hybrid double perovskite materials are not superior to the all-inorganic ones, and they are less stable than their all-inorganic counterparts.

In 2016, our group studied the effect of multiplicative interactions between bismuth triiodide and a layered organic–inorganic perovskite on the spectra absorption and photovoltaic performance of thin film solar cells. We prepared composite active layers with bismuth triiodide (BiI_3) and a layered perovskite $(CH_3NH_3)_3Bi_2I_9$ by a simple solution method. We found that the nano/macrostructures and morphology of BiI_3

have been modified due to the introduction of $(CH_3NH_3)_3Bi_2I_9$ with a large grain size. The absorption spectra of the composite active layers were enhanced. A shift in the conduction bands and the enlarged band gaps of the composite films were also observed. We achieved an enhancement of ca. 67% in the PCE of the fabricated solar cells due to the multiplicative interactions of the composite active layers.[46]

Bi-based perovskites are promising materials for the active layer of the solar cell due to their good stability and non-toxicity, as well as high absorption. However, the issue of the Bi perovskites is the low PCEs due to their relatively larger band gaps. It is essential to find a method of tuning the band gaps for improving the optical performance of the Bi perovskites.

4. Ge-based Perovskites

Ge, in the same group as Pb, is also considered to be the substitute for Pb. It has been widely used in the semi-conductor and Si-Ge hybrid solar cells fields. Earlier studies showed that the Ge-based perovskites could have solid-state properties similar to those of the Pb- and Sn-based perovskites.[47,48] In addition, the properties and applications of the Ge-based perovskite in the form of ABO_3 were previously studied.[49,50] However, studies of the Ge halide perovskite as a light absorber in the photovoltaic field have been limited until very recent.

In 2016, Sun et al. reported a computational study about the Ge-based perovskite using multiple DFT methods.[51] The mixed halide Ge perovskite with the form of $MAGeX_3$ (X = I, Br, Cl) was discussed. The calculated tolerance factors (TFs) of $MAGeX_3$ are 0.965 for I, 0.988 for Br, and 1.005 for Cl, while the TF of $MAPbI_3$ was calculated to be 0.834. These TFs were in the range of 0.97–1.03 for the ideal perovskite crystal model.[52] It was thus empirically argued that $MAGeX_3$ had an ideal perovskite structure. The band gap (E_g) of the $MAGeX_3$ perovskites were also estimated, and the E_g of $MAGeI_3$ was 1.61 eV, in contrast to 2.81 and 3.76 eV for the Br and Cl anions, respectively. The band gap data indicated that $MAGeI_3$ might have a higher potential than $MAGeBr_3$ and $MAGeCl_3$. They also carried out a detailed analysis of the density of the states, as well as the estimation of the effective masses when the elastic scattering within the lattice was minimized. The results demonstrated that $MAGeI_3$ had even better electron/hole transportation properties than Pb perovskites. Based on the obtained absorption coefficients, it was shown that $MAGeI_3$ also had a relatively good absorption in the 380–780 nm range of the spectrum. Although no practical experiment was carried out in this study, the potential of $MAGeX_3$ was observed.

Practical research was also carried out by Krishnamoorthy et al. in 2015.[53] They synthesized three kinds of $AGeI_3$ perovskites with difference cations, where the A site was Cs, CH_3NH_3 (MA), and $HC((NH_2)_2)$ (FA). The tolerance factor of the A cation became larger from Cs to MA and FA, indicating more distortion of the structures. Further TGA data supported their estimation. $CsGeI_3$ was more stable at the higher temperature of 350 °C than $MAGeI_3$ and $FAGeI_3$, which could only reach ca. 250 °C due to the decomposition of their organic cations at the A sites. The band gaps of the $AGeI_3$ (A: Cs, FA, MA) perovskites were estimated to be 1.63, 2.00, and 2.35 eV, respectively. The $CsGeI_3$ perovskite had a band gap similar to that of $MAPbI_3$; therefore, it was assessed to be a good substitute of Pb for PSCs applications. The other two Ge perovskites with larger band gaps could be considered to be candidates for achieving high open circuit voltages, and more suitable for tandem solar cell applications. The results suggested that we could tune the band gaps by changing the cation of the perovskites. The Krishnamoorthy group further constructed photovoltaic devices with the Ge perovskites $CsGeI_3$ and $MAGeI_3$ synthesized above. The devices showed the J_{sc} of 5.7 and 4 mA cm^{-2}, respectively. However, the V_{oc} of these devices were very low due to the poor solubility of these compounds in polar organic solvents. Also, the Ge^{2+} oxidation to Ge^{4+} was observed.

5. Alkaline-Earth Metal (Ca, Sr, Ba)-based Perovskites

Alkaline-earth metals (Ca, Sr, Ba) are also interesting materials for the substitution of Pb. The decision to employ alkaline-earth metals is stated to be based on Goldschmidt's rules of substitution, in combination with some quantum mechanical studies such as the bonding pattern analysis. Besides the theoretical suitability, the alkaline-earth metals and their compounds are usually of low cost, which is a natural advantage towards industrial applications.

Our group reported the partial substitution of Pb with Sr in 2015.[54] In this study, we synthesized Pb-Sr mixed perovskites with the formula of $MASr_XPb_{(1-X)}I_3$. We chose Sr based on the fact that Sr has an ion radius similar to that of Pb^+ (132 and 133 pm, respectively); therefore, it is considered to be able to replace Pb while bringing about no damaging structural change to the perovskite lattice. XRD results showed that the mixed perovskite possesses the typical perovskite structure. The SEM images of these mixed perovskites showed relatively large clusters on top of the perovskite film of the pure Pb-based perovskite, and when the Sr/Pb ratio increased, the cluster size decreased and eventually the clusters disappeared. This result indicated that the introduction of Sr could improve the morphology of the perovskite film by affecting the crystallization process and the deposition processor. However, it is also shown that at a higher Sr ratio (0.3:1), impurities will occur and decrease the electrical performance. It is also shown that for different Sr/Pb ratios, the band gaps of the perovskites also differ, and the change in the band gaps would directly reflect the change in absorption. The PCEs of these mixed PSCs were obtained to be much lower than that of Pb PSCs. Figure 4 showed some of the properties of this Sr/Pb mixed perovskite.

In 2015, Jacobsson et al. reported the theoretical study of a Sr perovskite, $MASrI_3$.[55] They employed coupled cluster singlet and doublet (CCSD) calculation to demonstrate that $MASrI_3$ could indeed have a crystal structure similar to $MAPbI_3$, and also DFT calculations suggest that $MASrI_3$ can be a close analogue with respect to the formation energy and cell parameters. However, the problem is that the estimated band gap of the $MASrI_3$ is too wide (3.6 eV), wider than most of the other substitutions discussed above. They also reported that synthesis attempts with conventional solution methods were not successful. The group tried out many alterations and changes, such as with different Sr sources (SrI_2, $SrCl_2$) and different solutions (DMF, DMSO, DMF/DMSO); however, the XRD results still showed that no perovskite was obtained. They thus concluded

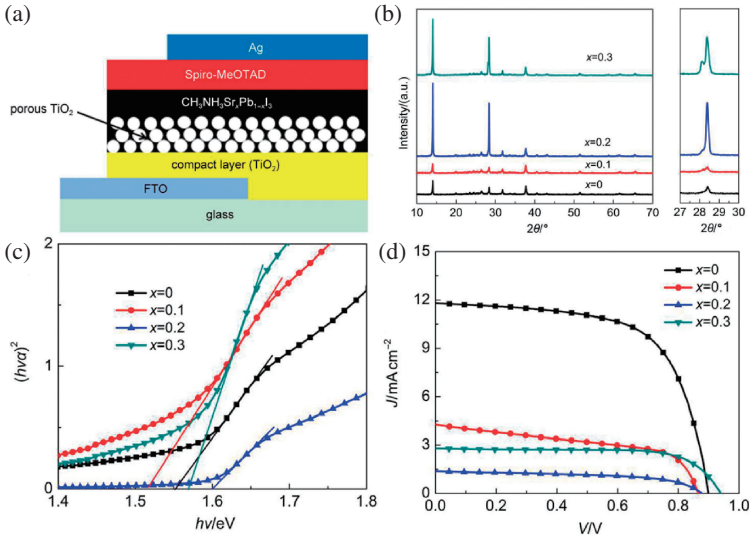

Figure 4. Device structure and properties of Sr/Pb mixed perovskite. (a) The device structure; (b) UV–vis absorption; (c) XRD pattern; (d) IPCE curve.[54]

that alternative synthesis routes, such as vapor phase synthesis or the layer-by-layer method, must be introduced in order to conduct further experimental studies.

Recently, Jacobsson et al. carried out another theoretical in-depth study of the Sr substitution and they expanded the study scope to not only Sr but also three alkaline-earth elements, i.e., Ca, Sr, and Ba.[56] They adopted general gradient approximation (GGA) exchange correlation function and Perdew–Burke–Ernzerhof (PBE) pseudopotential methods, which are presumably more precise when carrying out the crystal DFT calculations. They proposed that alkaline-earth element-based perovskites have a super cell structure consisting of 48 atoms in a tetragonal Bravais lattice. They estimated the formation energy for the Ba, Ca, Sr, and Pb perovskites, and the results showed that alkaline-earth metal perovskites have a slightly more negative formation energy compared to the Pb perovskites. They also found that the lattice constant of the alkaline-earth metal perovskites would slightly change with different ion radii compared to that of the Pb perovskites. These two facts suggested that the alkaline-earth metal perovskites could have a rather fine perovskite structure. It is postulated that the octahedron structure tilting in these alkaline-earth metal perovskites are mainly attributed to the atomic radii rather than the electronegativity, and the tilting has important effects on the band gaps and other properties. The estimated band gaps for the Ca, Sr, and Ba perovskites are 2.95, 3.6, and 3.3 eV, respectively. It is shown that the Ca, Sr, and Ba perovskites all have relatively large effective masses.

Our group also investigated the electronic properties of the lead-free halide double perovskites, Cs_2NaBX_6 (B = Sb and Bi; X = Cl, Br, and I) by first principle calculations to ascertain their potential application for solar energy conversion. These compounds were predicted to be of indirect band gap, which are similar to the very recently reported compound $Cs_2AgBiBr_6$. With treatment of the spin–orbital coupling, the band gaps for Cs_2NaSbI_6 and Cs_2NaBiI_6 were calculated to be 1.65 and 1.68 eV, respectively. Furthermore, the effective masses and absorption coefficients of the photocarriers were also calculated based on the PBE ground states. These results reveal the potential optoelectronic applications of these lead-free double perovskite materials.[57]

The crystal structure and the optoelectronic properties of alkaline-earth metal perovskites, in combination with the difficulty of fabrication, suggested that these alkaline-earth metal-based perovskites might not be good candidates for photoabsorbers. They are instead suggested to be potential good electron/hole selective materials. More detailed studies are still needed in this field.

6. Transition-metal-based Perovskites

While Sn, Bi, Sr, and Ge proved to possess very promising photovoltaic application potentials, other innovative alternatives also underwent intense studies. Transition metals were also considered as substitutes of Pb. The transition metal perovskites assume a 2D body-centered tetragonal layer structure, which allows the employment of more organic cation variations. In 2015, Cui et al. reported the synthesis of two cupric bromide perovskites, which are $(p\text{-}F\text{-}C_6H_5C_2H_4\text{-}NH_3)_2\text{-}CuBr_4$ and $(CH_3\text{-}(CH_2)_3NH_3)_2\text{-}CuBr_4$.[58] The estimated band gaps are 1.74 and 1.76 eV, respectively. The former achieved the PCE of 0.51% with $J_{sc} = 1.46\,mA\,cm^{-2}$, $V_{oc} = 0.87\,V$, and FF = 0.40, while the latter achieved the PCE of 0.63% with $J_{sc} = 1.78\,mA\,cm^{-2}$, $V_{oc} = 0.88$, and FF = 0.40.

Recent research by Cortecchia et al. reported fabricating a mixed halide perovskite with the structure of $MA_2CuI_XBr_{4-X}$.[59] Figure 5 shows the theoretical structure and the absorption of this Cu perovskite. This perovskite was reported to have a 2D structure mainly due to the smaller ionic radii of Cu, and its band gap can be tuned easily by adjusting the halogen composition. The study showed that when the halogen anions consisted of only bromine, the obtained perovskite had a low purity and was very sensitive to the atmospheric moisture. However, a very small amount of the chlorine additive (Cl:Br = 1:7) could

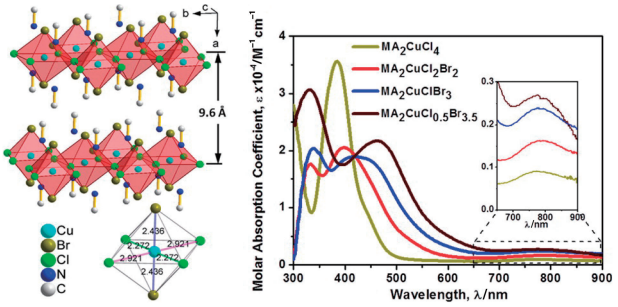

Figure 5. Structure and absorption of Cu-based perovskite.[59]

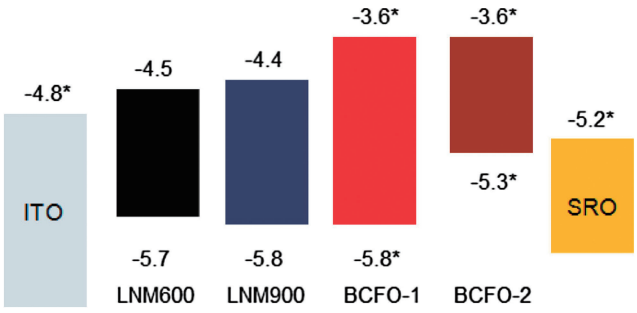

Figure 6. Band gaps of LNiMnO and BCrFeO.[61]

dramatically increase the magnitude of crystallization, as well as the stability in a humid environment. It is suggested that the ratio control is essential since fast crystallization would produce less uniform films. These findings are important when dealing with the common humid unstable problem of some perovskites. The Cu perovskites showed a wide absorption up to the NIR region, and the band gaps are rather large (2.8–3.0 eV). The reduction in the number of extra Cu^{2+} cations was found to be the major cause of the low PCE (only 0.01%). This material provides a new pathway for constructing perovskites, and it showed that the radical recombination of electronic pairs in the 2D structure would become an issue.

7. Ferroelectronic Perovskite Material La_2NiMnO_6

Ferroelectronic perovskite materials were previously used mainly targeting their magnetic properties. However, investigation of some ferroelectronic perovskites suggested that they have the potential to be employed as light absorbers. Moreover, they can be treated as a type of Pb-free perovskites. In 2009, Nechache et al. reported Bi_2CrFeO_6 as a light absorber, achieving the PCE of 8%.[60] However, such a material requires very complicated fabrication conditions with expensive methods such as pulsed-laser-involved physical vapor deposition.[44]

Our group focused on the study of La_2NiMnO_6, and carried out both theoretical and practical studies in 2015. We synthesized the La_2NiMnO_6 double perovskite by a simple solution Pechini method, which is mainly based on liquid-phase chemical reactions.[61] Both the monoclinic and rhombohedral structures of the La_2NiMnO_6 were obtained. We also found that the temperature can affect the crystal structure of La_2NiMnO_6. DFT and GGA+U method were employed to estimate the band gaps of La_2NiMnO_6 synthesized at 600 and 900 °C, obtaining 1.2 and 1.4 eV, respectively. These results are lower than that of the $LaMnO_3$ single perovskite (1.7–2.0 eV). Figure 6 showed the calculated band gaps of La_2NiMnO_6 and Bi_2CrFeO_6.

8. Summary

In this review, we introduced the current advancements in Pb-free perovskite materials aiming at photovoltaic applications. The developed substitutes for Pb included Sn, Bi, Sr, Ge, Cu, and some double perovskites. We have summarized various Pb-free perovskite solar cells and their performances in Table 1.

Among them, the Sn-based perovskite achieved the highest performance. However, the stability and toxic issues still remain.

Table 1. Pb-free perovskites optoelectronic properties summary

Perovskites	PCE /%	V_{oc} /V	J_{sc} /mA cm^{-2}	FF	Band gap /eV
$MAPb_{0.85}Sn_{0.15}I_3$[16]	10.10	0.76	19.12	0.66	N/A
$MAPb_{0.75}Sn_{0.25}I_3$[17]	7.37	0.73	15.82	0.64	1.17
$MAPb_{0.85}Sn_{0.15}I_{3-v}Cl_v$[17]	9.77	0.76	19.10	0.66	1.38
$MA_{0.5}FA_{0.5}Pb_{0.75}Sn_{0.25}I_3$[18]	14.35	0.82	22.44	0.78	1.33
$MASnI_3$[21]	6.50	0.88	16.8	0.42	1.23
$MAPb_{0.5}Sn_{0.5}I_3$[14]	4.18	0.32	19.88	0.37	1.28
$MAPb_{0.5}Sn_{0.5}I_3$[15]	10.00	0.69	22.80	0.635	1.12
$MAPb_{0.5}Sn_{0.5}I_3$[19]	13.60	0.75	36.30	0.688	1.18
$(MAPbI_3)_{0.4}(FASnI_3)_{0.6}$[20]	15.08	0.795	26.86	0.706	1.20
$FASnI_3$[22]	6.22	0.465	22.07	0.607	1.40
$FASnI_3$[23]	4.00	0.29	24.50	0.55	N/A
$CsSnI_3$[24]	4.81	0.38	25.71	0.49	N/A
$MASnBr_3$[26]	1.12	0.50	4.27	0.49	2.30
$MASnI_3$[27]	1.86	0.27	17.80	0.39	1.27
$MASnI_3$[28]	2.14	0.45	11.82	0.40	N/A
$A_3Bi_2I_9$ (A = MA, Cs)[31]	0.12	0.68	0.52	0.33	2.1
	1.09	0.85	2.15	0.60	2.2
$MA_3Bi_2I_9$[37]	0.31	0.51	0.94	0.61	N/A
$MA_3Bi_2I_9$[38]	0.082	0.69	0.37	0.32	N/A
$MAGeX_3$ (X = Cl, Br, I)[51]	Not reported			0.59	3.76
				0.53	2.81
				0.66	1.61
AGeI (A = Cs, MA)[53]	0.11	0.74	5.70	0.27	1.60
	0.20	1.50	4.00	0.30	2.00
$MASr_XPb_{(1-X)}I_3$	1.97	0.87	4.32	0.53	N/A
(X = 0.1, 0.2, 0.3)[55]	0.69	0.88	1.34	0.59	N/A
	1.93	0.94	2.80	0.73	N/A
$MABI_3$ (B = Ca, Sr, Ba)[56]	Not reported				2.90, 3.60, 3.30
$CsNaMI_6$ (M = Sb, Bi)[57]	Not reported				1.65, 1.68
(*p*-F-$C_6H_5C_2H_4$-NH_3)$_2$-$CuBr_4$[58]	0.51	0.87	1.46	0.40	1.74
$(CH_3(CH_2)_3NH_3)_2$-$CuBr_4$[58]	0.63	0.88	1.78	0.40	1.76
$MA_2CuI_XBr_{(4-X)}$	0.0017	0.29	<0.01	0.28	1.80
(X = 0.5, 1, 2)[59]	N/A				1.90
	0.017	0.256	<0.01	0.32	2.12

On the other hand, Bi-based perovskites are not only much less toxic, but also show a remarkably improved stability than the Pb-based perovskites, but the problem is low PCE.

Ge, Sr, and Cu were predicted by theoretical calculation to be good substitutes. However, practical experiments encountered unexpected difficulties. Moreover, the high cost of both the raw material and fabrication methods suggested that further investigations should be carried out. Despite the fact that the Ge

perovskites have potential applications, the cost of the Ge element could be one great challenge to overcome. The Sr-based perovskites encountered an issue that they are difficult to synthesize experimentally. Cu was recently studied; the Cu-based perovskites are more stable than the Sn-based and Ge-based perovskites; unfortunately, the devices only produce very low PCEs. A new technique breakthrough is needed to develop new Pb-free perovskite materials.

Although lead-free perovskite-based solar cells hold the promise of next-generation photovoltaic devices, a low efficiency and inadequate stability remain as major challenges. In addition, the overall performances of the lead-free PSCs are still relatively low compared to those of the lead-based PSCs. Much more research effort is expected in the area of developing new materials and improving the performance of the solar cells, which make PSCs as the real green and low-cost next-generation technology for sustainable solar energy conversion.

References

1 G. Hodes, *Science* **2013**, *342*, 317.
2 A. Kojima, K. Teshima, Y. Shirai, T. Miyasaka, *J. Am. Chem. Soc.* **2009**, *131*, 6050.
3 J.-H. Im, C.-R. Lee, J.-W. Lee, S.-W. Park, N.-G. Park, *Nanoscale* **2011**, *3*, 4088.
4 H.-S. Kim, C.-R. Lee, J.-H. Im, K.-B. Lee, T. Moehl, A. Marchioro, S.-J. Moon, R. Humphry-Baker, J.-H. Yum, J. E. Moser, M. Grätzel, N.-G. Park, *Sci. Rep.* **2012**, *2*, 591.
5 T. Miyasaka, *Chem. Lett.* **2015**, *44*, 720.
6 M. M. Lee, J. Teuscher, T. Miyasaka, T. N. Murakami, H. J. Snaith, *Science* **2012**, *338*, 643.
7 Q. Dong, Y. Fang, Y. Shao, P. Mulligan, J. Qiu, L. Cao, J. Huang, *Science* **2015**, *347*, 967.
8 J. Feng, B. Xiao, *J. Phys. Chem. C* **2014**, *118*, 19655.
9 S. K. Pathak, A. Abate, P. Ruckdeschel, B. Roose, K. C. Gödel, Y. Vaynzof, A. Santhala, S.-I. Watanabe, D. J. Hollman, N. Noel, A. Sepe, U. Wiesner, R. Friend, H. J. Snaith, U. Steiner, *Adv. Funct. Mater.* **2014**, *24*, 6046.
10 S. K. Pathak, A. Abate, T. Leijtens, D. J. Hollman, J. Teuscher, L. Pazos, P. Docampo, U. Steiner, H. J. Snaith, *Adv. Energy Mater.* **2014**, *4*, 1301667.
11 T. A. Berhe, W.-N. Su, C.-H. Chen, C.-J. Pan, J.-H. Cheng, H.-M. Chen, M.-C. Tsai, L.-Y. Chen, A. A. Dubale, B.-J. Hwang, *Energy Environ. Sci.* **2016**, *9*, 323.
12 C. C. Stoumpos, C. D. Malliakas, M. G. Kanatzidis, *Inorg. Chem.* **2013**, *52*, 9019.
13 H. D. Kim, Y. Miyamoto, H. Kubota, T. Yamanari, H. Ohkita, *Chem. Lett.* **2017**, *46*, 253.
14 Y. Ogomi, A. Morita, S. Tsukamoto, T. Saitho, N. Fujikawa, Q. Sheng, T. Toyoda, K. Yoshino, S. S. Pandey, T. Ma, S. Hayase, *J. Phys. Chem. Lett.* **2014**, *5*, 1004.
15 G. Lin, Y. Lin, H. Huang, R. Cui, X. Guo, B. Liu, J. Dong, X. Guo, B. Sun, *Nano Energy* **2016**, *27*, 638.
16 F. Hao, C. C. Stoumpos, R. P. H. Chang, M. G. Kanatzidis, *J. Am. Chem. Soc.* **2014**, *136*, 8094.
17 F. Zuo, S. T. Williams, P.-W. Liang, C.-C. Chueh, C.-Y. Liao, A. K.-Y. Jen, *Adv. Mater.* **2014**, *26*, 6454.
18 Z. Yang, A. Rajagopal, C.-C. Chueh, S. B. Jo, B. Liu, T. Zhao, A. K.-Y. Jen, *Adv. Mater.* **2016**, *28*, 8990.
19 Y. Li, W. Sun, W. Yan, S. Ye, H. Rao, H. Peng, Z. Zhao, Z. Bian, Z. Liu, H. Zhou, C. Huang, *Adv. Energy Mater.* **2016**, *6*, 1601353.
20 W. Liao, D. Zhao, Y. Yu, N. Shrestha, K. Ghimire, C. R. Grice, C. Wang, Y. Xiao, A. J. Cimaroli, R. J. Ellingson, N. J. Podraza, K. Zhu, R.-G. Xiong, Y. Yan, *J. Am. Chem. Soc.* **2016**, *138*, 12360.
21 N. K. Noel, S. D. Stranks, A. Abate, C. Wehrenfennig, S. Guarnera, A.-A. Haghighirad, A. Sadhanala, G. E. Eperon, S. K. Pathak, M. B. Johnston, A. Petrozza, L. M. Herz, H. J. Snaith, *Energy Environ. Sci.* **2014**, *7*, 3061.
22 W. Liao, D. Zhao, Y. Yu, C. R. Grice, C. Wang, A. J. Cimaroli, P. Schukz, W. Meng, K. Zhu, R.-G. Xiong, Y. Yan, *Adv. Mater.* **2016**, *28*, 9333.
23 S. J. Lee, S. S. Shin, Y. C. Kim, D. Kim, T. K. Ahn, J. H. Noh, J. Seo, S. I. Seok, *J. Am. Chem. Soc.* **2016**, *138*, 3974.
24 T.-B. Song, T. Yokoyama, S. Aramaki, M. G. Kanatzidis, *ACS Energy Lett.* **2017**, *2*, 897.
25 T. Yokoyama, T.-B. Song, D. H. Cao, C. C. Stoumpos, S. Aramaki, M. G. Kanatzidis, *ACS Energy Lett.* **2017**, *2*, 22.
26 M.-C. Jung, S. R. Raga, Y. Qi, *RSC Adv.* **2016**, *6*, 2819.
27 T. Yokoyama, D. H. Cao, C. C. Stoumpos, T.-B. Song, Y. Sato, S. Aramaki, M. G. Kanatzidis, *J. Phys. Chem. Lett.* **2016**, *7*, 776.
28 T. Fujihara, S. Terakawa, T. Matsushima, C. Qin, M. Yahiro, C. Adachi, *J. Mater. Chem. C* **2017**, *5*, 1121.
29 A. Babayigit, D. D. Thanh, A. Ethirajan, J. Manca, M. Muller, H.-G. Boyen, B. Conings, *Sci. Rep.* **2016**, *6*, 18721.
30 H. Zhou, Q. Chen, G. Li, S. Luo, T. Song, H.-S. Duan, Z. Hong, J. You, Y. Liu, Y. Yang, *Science* **2014**, *345*, 542.
31 B.-W. Park, B. Philippe, X. Zhang, H. Rensmo, G. Boschloo, E. M. J. Johansson, *Adv. Mater.* **2015**, *27*, 6806.
32 R. L. Z. Hoye, R. E. Brandt, A. Osherov, V. Stevanović, S. D. Stranks, M. W. B. Wilson, H. Kim, A. J. Akey, J. D. Perkins, R. C. Kurchin, J. R. Pointdexter, E. N. Wang, M. G. Bawendi, V. Bulović, T. Buonassisi, *Chem.—Eur. J.* **2016**, *22*, 2605.
33 K. Eckhardt, V. Bon, J. Getzschmann, J. Grothe, F. M. Wisser, S. Kaskel, *Chem. Commun.* **2016**, *52*, 3058.
34 Y.-Y. Sun, J. Shi, J. Lian, W. Gao, M. L. Agiorgousis, P. Zhang, S. Zhang, *Nanoscale* **2016**, *8*, 6284.
35 T. Baikie, Y. Fang, J. M. Kadro, M. Schreyer, F. Wei, S. G. Mhaisalkar, M. Graetzel, T. J. White, *J. Mater. Chem. A* **2013**, *1*, 5628.
36 F. Hong, B. Saparov, W. Meng, Z. Xiao, D. B. Mitzi, Y. Yan, *J. Phys. Chem. C* **2016**, *120*, 6435.
37 A. Kulkarni, T. Singh, M. Ikegami, T. Miyasaka, *RSC Adv.* **2017**, *7*, 9456.
38 T. Okano, Y. Suzuki, *Mater. Lett.* **2017**, *191*, 77.
39 C. Ran, Z. Wu, J. Xi, F. Yuan, H. Dong, T. Lei, X. He, X. Hou, *J. Phys. Chem. Lett.* **2017**, *8*, 394.
40 Z. Xiao, W. Meng, J. Wang, Y. Yan, *ChemSusChem* **2016**, *9*, 2628.
41 G. Volonakis, M. R. Filip, A. A. Haghighirad, N. Sakai, B. Wenger, H. J. Snaith, F. Giustino, *J. Phys. Chem. Lett.* **2016**, *7*, 1254.
42 A. H. Slavney, T. Hu, A. M. Lindenberg, H. I. Karunadasa, *J. Am. Chem. Soc.* **2016**, *138*, 2138.
43 M. R. Filip, S. Hillman, A. A. Haghighirad, H. J. Snaith, F. Giustino, *J. Phys. Chem. Lett.* **2016**, *7*, 2579.
44 F. Wei, Z. Deng, S. Sun, F. Xie, G. Kieslich, D. M. Evans, M. A. Carpenter, P. D. Bristowe, A. K. Cheetham, *Mater.*

Horiz. **2016**, *3*, 328.
45 F. Wei, Z. Deng, S. Sun, F. Zhang, D. M. Evans, G. Kieslich, S. Tominaka, M. A. Carpenter, J. Zhang, P. D. Bristowe, A. K. Cheetham, *Chem. Mater.* **2017**, *29*, 1089.
46 C. Lan, J. Luo, S. Zhao, C. Zhang, W. Liu, S. Hayase, T. Ma, *J. Alloys Compd.* **2017**, *701*, 834.
47 K. Yamada, K. Isobe, T. Okuda, Y. Furukawa, *Z. Naturforsch., A: Phys. Sci.* **1994**, *49*, 258.
48 S. J. Clark, J. D. Donaldson, J. A. Harvey, *J. Mater. Chem.* **1995**, *5*, 1813.
49 H.-R. Fuh, Y.-P. Liu, S.-H. Chen, Y.-K. Wang, *J. Alloys Compd.* **2013**, *547*, 126.
50 M. F. M. Taib, M. K. Yaakob, F. W. Badrudin, M. S. A. Rasiman, T. I. T. Kudin, O. H. Hassan, M. Z. A. Yahya, *Integr. Ferroelectr.* **2014**, *155*, 23.
51 P.-P. Sun, Q.-S. Li, L.-N. Yang, Z.-S. Li, *Nanoscale* **2016**, *8*, 1503.
52 M. A. Green, A. Ho-Baillie, H. J. Snaith, *Nat. Photonics* **2014**, *8*, 506.
53 T. Krishnamoorthy, H. Ding, C. Yan, W. L. Leong, T. Baikie, Z. Zhang, M. Sherburne, S. Li, M. Asta, N. Mathews, S. G. Mhaisalkar, *J. Mater. Chem. A* **2015**, *3*, 23829.
54 X.-G. Bai, Y.-T. Shi, K. Wang, Q.-S. Dong, Y.-J. Xing, H. Zhang, L. Wang, T.-L. Ma, *Wuli Huaxue Xuebao* **2015**, *31*, 285.
55 T. J. Jacobsson, M. Pazoki, A. Hagfeldt, T. Edvinsson, *J. Phys. Chem. C* **2015**, *119*, 25673.
56 M. Pazoki, T. J. Jacobsson, A. Hagfeldt, G. Boschloo, T. Edvinsson, *Phys. Rev. B* **2016**, *93*, 144105.
57 S. Zhao, C. Lan, S. S. Pandy, S. Hayase, T. L. Ma, *J. Phys. Chem. C* **2016**, submitted.
58 X.-P. Cui, K.-J. Jiang, J.-H. Huang, Q.-Q. Zhang, M.-J. Su, L.-M. Yang, Y.-L. Song, X.-Q. Zhou, *Synth. Met.* **2015**, *209*, 247.
59 D. Cortecchia, H. A. Dewi, J. Yin, A. Bruno, S. Chen, T. Baikie, P. P. Boix, M. Grätzel, S. Mhaisalkar, C. Soci, N. Mathews, *Inorg. Chem.* **2016**, *55*, 1044.
60 R. Nechache, C. Harnagea, L.-P. Carignan, O. Gautreau, L. Pintilie, M. P. Singh, D. Ménard, P. Fournier, M. Alexe, A. Pignolet, *J. Appl. Phys.* **2009**, *105*, 061621.
61 C. Lan, S. Zhao, T. Xu, J. Ma, S. Hayase, T. Ma, *J. Alloys Compd.* **2016**, *655*, 208.